Ecological Engineering 88 (2016) 237–241

Contents lists available at ScienceDirect

Ecological Engineering

journal homepage: www.elsevier.com/locate/ecoleng

Short communication

Isotherm and kinetic study on Ni(II) and Pb(II) biosorption by the fern *Asplenium nidus* L.

D.M.R.E.A. Dissanayake[a,b], W.M.K.E.H. Wijesinghe[a,b], S.S. Iqbal[c], N. Priyantha[b], M.C.M. Iqbal[a,*]

[a] Plant Biology Laboratory, National Institute of Fundamental Studies, Hanthana Road, Kandy, Sri Lanka
[b] Postgraduate Institute of Science, University of Peradeniya, Peradeniya, Sri Lanka
[c] Department of Chemistry, Faculty of Natural Sciences, Open University Sri Lanka, Nawala, Sri Lanka

ARTICLE INFO

Article history:
Received 8 June 2015
Received in revised form
16 December 2015
Accepted 17 December 2015

Keywords:
Biosorption
Kinetic modeling
Isotherm modeling
Pb(II)
Ni(II)

ABSTRACT

The extent of biosorption of Pb(II) and Ni(II) by dried leaves of the fern *Asplenium nidus* depends on experimental conditions, such as initial pH, initial concentration, contact time and shaking speed. Kinetic data were fitted to pseudo first order, pseudo second order, intraparticle diffusion and Elovich models. Isotherm data were fitted to two-parameter and three-parameter isotherm models. *A. nidus* adsorbed 58% of Ni(II) and 95% of Pb(II) after 30 min and 75 min, respectively, under the experimental conditions provided. The protonated biosorbent adsorbed 75% of Ni(II) after 30 min. Kinetic data fitted the pseudo second order model and the intraparticle diffusion model showed that intraparticle diffusion is not the only process that governs the adsorption process. Isotherm studies showed that Langmuir–Freundlich isotherm model explains the adsorption process well.

1. Introduction

Both nickel and lead are heavily used in industries. Discharge of these metal bearing effluents thus contaminates the environment. As exposure to these heavy metals would induce health problems, it is essential to remove Pb(II) and Ni(II) from contaminated water systems before they enter waterways, and subsequently the food chain.

Most large-scale industries have installed end-pipe treatment systems, such as ion-exchange (Inglezakis and Loizidou, 2007; Inglezakis et al., 2002), membrane filtration (Molinari et al., 2004), chemical precipitation and oxidation (Dickenson et al., 2009; Mitra et al., 2011) and electrochemical methods (Rana et al., 2004). These methods are not only capital intensive but also require trained personnel. An alternative for these methods is the adsorption of heavy metals using natural adsorbents. Biosorption uses non-living biological materials as adsorbents to remove pollutants from aqueous environments (Volesky, 2003). Depending on the cell wall composition of the plant, the functional groups of the biosorbent responsible for adsorption would vary. Natural adsorbents that have been studied include aquatic plants, such as *Hydrilla* (Chathuranga et al., 2014; Huang et al., 2009), *Cabomba* (Chathuranga et al., 2013), tea factory waste (Amarasinghe and Williams, 2007; Jacques et al., 2007), fungal biomasses (Akar et al., 2013; Bai and Abraham, 2003) and marine algae (Volesky et al., 2003). Although ferns, as a biosorbent, has been reported (Ho, 2005; Ho and Wang, 2008), detailed kinetics and isothermal studies were not given sufficient attention.

In this study, the tropical fern *Asplenium nidus*, an ornamental plant, was used as a novel biological material to prepare a cost-effective biosorbent for the removal of Ni(II) and Pb(II) from aqueous environments. Simple modifications were done to enhance the biosorption capacity of the biosorbent. Batch adsorption models were studied to understand the mechanism of the biosorption process and to develop practical applications. Linearized pseudo first order, pseudo second order, intraparticle diffusion model and Elovich model were applied to understand the adsorption mechanism. Further application of both linear and non-linear forms of Langmuir, Freundlich, Dubinin–Radushkevich and Temkin isotherm models was highlighted.

2. Materials and methods

2.1. Preparation of the biosorbent

Fresh plant leaves of *A. nidus*, collected from domestic gardens, were washed with tap water followed by deionized water. They

* Corresponding author.
E-mail address: mcmif2003@yahoo.com (M.C.M. Iqbal).

http://dx.doi.org/10.1016/j.ecoleng.2015.12.028
0925-8574/

were air dried for 48 h and oven dried at 80 °C for 48 h. Dried fern leaves (biosorbent) were ground and sieved to obtain a particle size fraction between 250 μm and 350 μm. For the protonation of the biosorbent, 10.0 g of dried *A. nidus* was mixed with 500.0 mL of 0.1 mol L^{-1} HNO_3. The suspension was stirred at 200 rpm for 6.0 h, filtered and washed with deionized water to remove the excess acid. The biosorbent was then air dried for 48 h and oven dried at 80 °C for 48 h.

2.2. Chemicals and instrumentation

All the chemicals used were of analytical grade from BDH Chemicals, England and Sigma–Aldrich Chemicals, USA. Standard test solutions of $Pb(NO_3)_2$ and $NiCl_2{\cdot}6H_2O$ were prepared in deionized distilled water. The initial pH of the solutions was adjusted using either HNO_3 or NaOH.

The Pb(II) and Ni(II) concentrations were determined using a flame atomic absorption spectrophotometer Model GBC-933AA. Biosorbent-metal suspensions were shaken on an orbital shaker (Gallenkamp).

Fourier transform infrared (FTIR) spectra of the native and metal-loaded samples were obtained from a FTIR spectrophotometer (model Thermo Science NICOLET 6700). The sample disks were prepared using anhydrous KBr and the spectral range varied from 400 cm^{-1} to 4000 cm^{-1}.

2.3. Experimental parameters on the extent of biosorption

Biosorbent (0.200 g) was introduced separately into 100.0 mL each of 5.0 mg L^{-1} Pb(II) and Ni(II) solution at pH 5.0 and at ambient temperature (27 °C). The suspensions were shaken at a speed of 100 rpm. Suspensions were removed from the shaker at predetermined time intervals, filtered and the filtrate was analyzed for residual metal content. The same experiment was repeated at optimum shaking time, but changing the initial solution pH from 1.0 to 7.0 to determine the effect of initial pH.

Metal solutions whose concentration varied from 1.0 mg L^{-1} to 20 mg L^{-1} at pH 5.0 were used to determine the effect of initial metal ion concentration on biosorption.

Similarly 0.200 g of dried biosorbent was introduced in to 100.0 mL of 5.0 mg L^{-1} Ni(II) and Pb(II) solutions separately at pH 5.0 and 27 °C, and suspensions were shaken at different speeds (60, 100, 140 and 180 rpm) to determine the effect of shaking speed.

2.4. Analysis of batch adsorption data

The absorption percentage and the adsorption amount (q) were calculated using Eqs. (1) and (2), respectively,

$$A\% = \frac{(C_i - C_f)}{C_i} \times 100\% \quad (1)$$

$$q = \frac{(C_i - C_f)}{M} \times V \quad (2)$$

where C_i is the initial metal concentration and C_f is the final metal concentration of the solution (mg L^{-1}). V (L) is the volume of metal solution and M (mg) is the amount of biomass used.

Biosorption process was modeled using linearized pseudo first order (Eq. (3)) and pseudo second order (Eq. (4)) kinetic models:

$$\ln(q_e - q_t) = \ln q_e - \ln k_1 t \quad (3)$$

$$\frac{1}{q_t} = \frac{1}{k_2 q_e^2 t} + \frac{1}{q_e} \quad (4)$$

where q_e and q_t denote the amounts of Pb(II) and Ni(II) ions adsorbed per unit mass of the sorbent (mg g^{-1} dry biomass) at equilibrium and at time t, respectively, k_1 and k_2 are the pseudo

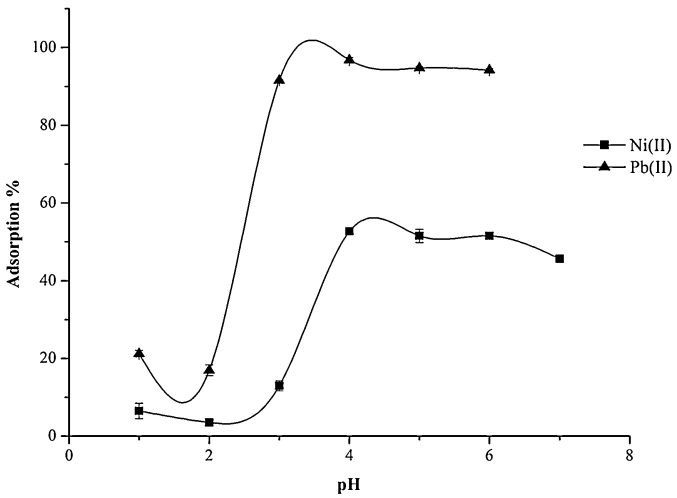

Fig. 1. Effect of pH on biosorption of Pb(II) and Ni(II) by 0.2 g of *A. nidus* biosorbent (initial metal concentration = 5.0 mg L^{-1}, temperature = 27 °C, shaking speed 100 rpm, n = 3).

first order rate constant (min^{-1}) and the pseudo second order rate constant (g mg^{-1} min^{-1}), respectively. The amount of metal ions adsorbed on to the biosorbent was calculated using Eq. (1).

The compatibility of adsorption data with the intraparticle diffusion model was determined using Eq. (5):

$$q_t = k_i t^{0.5} \quad (5)$$

where k_i is the intraparticle rate constant (mg g^{-1} $min^{-0.5}$).

The compatibility of kinetics data adsorption with the Elovich model was determined using Eq. (6):

$$q_t = \left(\frac{1}{\beta}\right) \ln(\alpha\beta) + \left(\frac{1}{\beta}\right) \ln t \quad (6)$$

where α is the initial Ni(II) adsorption rate (mg g^{-1} min^{-1}) and β is the desorption constant (g mg^{-1}).

The non-linear and linear forms used in the investigation for the validity of each isotherm are given in Table 1.

3. Results and discussion

3.1. Effect of contact time and settling time

The adsorption of Pb(II) and Ni(II) increased with increasing time to a maximum and remained the same thereafter. Pb(II) was adsorbed to a maximum of 95% after 75 min. After equilibrium was reached, there was no significant change in adsorption. The maximum adsorption of 58% for Ni(II) took 30 min. However, the adsorbent after protonation adsorbed 76% of Ni(II) after 30 min. These times for maximum adsorption were selected as the optimum contact time for further experiments.

Protonation of the biosorbent surface has increased the H^+ ions on the surface, which can be rapidly exchanged with Ni(II) ions in the solution as shown by the increased adsorption of Ni(II) after protonation. A similar observation was reported for Cr(III) adsorption by *Cabomba caroliniana* (Chathuranga et al., 2013). This is an indication that the biosorption process involves an ion exchange mechanism.

3.2. Effect of initial solution pH, initial metal concentration and shaking speed

The low level of adsorption observed at low pH is probably due to competitive ion-exchange of mobile H^+ ions with metal ions to bind

Table 1
Non-linear and linear forms of isotherm models.

Name of the isotherm	Nonlinear form	Linear form
Langmuir isotherm	$q_e = \frac{q_0 b C_e}{1+bC_e}$	$\frac{1}{q_e} = \frac{1}{q_0} + \frac{1}{bq_0 C_e}$
Freundlich isotherm	$q_e = k_f C_e^{1/n}$	$\ln q_e = \ln k_f + \frac{1}{n} \ln C_e$
Temkin isotherm	$q_e = \frac{RT}{b_T} \ln A_T C_e$	$q_e = \frac{R_T}{B_T} \ln A_T C_e$
Dubinin–Raduskevich	$q_e = q_0 \exp\left\{-\left[\frac{RT \ln(C_s/C_e)}{E}\right]^2\right\}$	$\ln q_e = \ln q_s - k_{ad}\varepsilon^2$
Langmuir–Freundlich isotherm	$q_e = \frac{q_{0(k_a C_e)^n}}{(k_a C_e)^n+1}$	
Redlich–Peterson isotherm	$q_e = \frac{k_{RP} C_e}{1+a_{RP} C_e^{\beta}}$	$\ln\left(k_{RP}\frac{C_e}{q_e} - 1\right) = \beta \ln C_e + \ln a_{RP}$

q_e: amount of metal ions adsorbed per unit mass of the biosorbent (mg g^{-1}), q_0: maximum adsorption capacity (mg g^{-1}), C_e: residual metal ion concentration (mg L^{-1}), b: adsorption coefficient, k_f: Freundlich isotherm constant, n: adsorption intensity, R: Universal gas constant (8.314 J mol^{-1} K^{-1}), T: absolute temperature (K), b_T: Temkin isotherm constant, A_T: Temkin isotherm equilibrium binding constant (L g^{-1}), C_s: saturation concentration, $E = \left[1/\sqrt{2\beta}\right]$: mean free energy per molecule of adsorbent, β: Dubinin–Radushkevich constant (mol^2 J^{-2}), k_a and k_{RP}: affinity constant for adsorption (L mg^{-1}), β: index of heterogeneity, a_{RP}: Redlich–Peterson isotherm constant.

with functional groups on the biosorbent (Malkoc and Nuhoglu, 2006), resulting in positively charged biosorbent surface (Fig. 1). A low initial pH of the solution would also damage the biosorbent structure affecting its adsorption capacity (Volesky, 2003). The optimum pH of 4–6, enabled a maximum adsorption of 94% for Pb(II) and 51% for Ni(II) (Fig. 1). Similar observations were reported for Pb(II) adsorption on to *Hydrilla verticillata* (Chathuranga et al., 2014). After pH 6, the Pb(II) solution forms $Pb(OH)_2$ and adsorption is constant while $Ni(OH)_2$ is formed after pH 7 giving a maximum adsorption of 51%.

When the metal concentration increased, the adsorbed amount also increased as expected. However, a mass of 0.200 g *A. nidus* and 5.0 mg L^{-1} concentration was selected for future experiments. On the other hand, the increase in shaking speed from 60 to 180 rpm did not show significant variation in adsorption. Without shaking the system, 70% adsorption was observed for Pb(II) by the biosorbent. This indicates a strong affinity for Pb(II) by the biosorbent. Similar observations on biosorption of Pb(II) of over 90% were reported in previous studies (Chathuranga et al., 2014; Mondal, 2009; Taty-Costodes et al., 2005).

3.3. Kinetics of the adsorption process

The values of the rate constants k_1 and k_2, and q_e obtained from each linearized model are presented in Table 2. Although there was no large difference between the R^2 values for each model, the experimental q_e value is closer to the theoretical value for the pseudo second order model. Therefore, the rate of the biosorption process depends on both the metal ion concentration and the concentration of biosorbent (Jacques et al., 2007; Shroff and Vaidya, 2011).

In addition to the above kinetic models, the intraparticle diffusion and Elovich models were used to understand the mechanism of the adsorption process. The intraparticle diffusion model assumes that intraparticle diffusion is the only rate-controlling process. The Elovich model describes the heterogeneous chemisorption of the adsorbate on to the solid adsorbent. The non-zero intercept of the plot of q_t vs. $t^{0.5}$ indicates that intraparticle diffusion is not the only rate-controlling mechanism in Pb(II) and Ni(II) adsorption (Chathuranga et al., 2014). Higher intraparticle diffusion constant for Ni(II) adsorption (0.09 mg g^{-1} min$^{0.5}$) than that of Pb(II) adsorption (0.08 mg g^{-1} min$^{0.5}$, Table 2) indicates that the adsorption of Ni(II) is faster than that of Pb(II). As the plot of the experimental data for the Elovich equation gave a high correlation coefficient (>0.91, Table 2), it is predicted that the adsorption system is highly heterogeneous (Ho and McKay, 2002).

4. Isotherm studies

4.1. Two parameter isotherm models

Two parameter isotherm model analysis for Pb(II) and Ni(II) adsorption on *A. nidus* biosorbent suggests that the adsorption process follows Langmuir and Freundlich isotherm models (Fig. 1) with high R^2 values (Table 3). The adsorption intensity for Langmuir isotherm (R_L) values for Ni(II) and Pb(II) varied from 0.06 to 0.48 and 0.027 to 0.23, respectively. Therefore, both Pb(II) and Ni(II) adsorption processes are favorable ($0 < R_L < 1$) (Foo and Hameed, 2010). The monolayer adsorption capacity (q_0) for Pb(II) adsorption was higher (12.24 mg g^{-1}) than that for Ni(II) (9.20 mg g^{-1}, Table 3). In the Freundlich isotherm equation, $1/n$ is an expression of heterogeneity of the surface or the adsorption intensity where, as $1/n$ approaches zero, the surface is more heterogeneous (Foo and Hameed, 2010). In this study, $1/n$ value for Ni(II) adsorption was 0.74, and that for Pb(II) adsorption was 0.63 (Table 3), which indicates the heterogeneity of the biosorbent surface.

The FTIR study of the biosorbent showed several peak positions of different functional groups (–OH (3432 cm^{-1}), primary amines of N–H (1643 cm^{-1}) and C–O stretching of primary alcohols (1107 cm^{-1})) on the biosorbent surface, further indicating the heterogeneity of the biosorbent surface.

Due to different behavior of the Langmuir and Freundlich models (heterogeneity, and R^2), the data were fitted to Temkin and

Table 2
Calculated kinetic model parameters of different kinetic models for biosorption of Pb(II) and Ni(II) on to *A. nidus* biosorbent (initial metal concentration 5.0 mg L^{-1}, initial pH 5.0, shaking speed = 100 rpm, temperature 27 °C, $n = 3$).

Model	Pseudo first order		Pseudo second order		Intraparticle diffusion model		Elovich	
Metal	Ni(II)	Pb(II)	Ni(II)	Pb(II)	Ni(II)	Pb(II)	Ni(II)	Pb(II)
Slope	−0.06	−0.04	1.35	0.54	0.09	0.08	0.19	0.21
Intercept	−0.71	−0.70	0.81	0.41	0.74	1.86	0.62	1.63
Rate constant (k)	1.06 min^{-1}	1.04 min^{-1}	0.49 g mg^{-1} min^{-1}	0.31 g mg^{-1} min^{-1}	0.091 mg g^{-1} min$^{0.5}$	0.080 mg g^{-1}	5.33 g mg^{-1}	4.86 g mg^{-1}
q_e (Exp)	1.30	2.45	1.30	2.45	NA	NA	NA	NA
q_e (Theo)	0.49	0.50	1.23	2.46	NA	NA	NA	NA
R^2	0.993	0.933	0.987	0.965	0.972	0.817	0.918	0.931

NA: not applicable.

Table 3
Adsorption isotherm parameters for Pb(II) and Ni(II) adsorption on to 0.2 g of *A. nidus* leaves (temperature = 27 °C, pH = 5.0, shaking speed = 100 rpm, $n = 3$). See text for abbreviations.

Metal	Model	k	q_0	n	E	A_T	b_T	a_{RP}	C_s	R^2	χ^2
Ni(II)	Langmuir	0.07	9.20	NA	NA	NA	NA	NA	NA	0.847	0.414
	Freundlich	0.69	NA	1.34	NA	NA	NA	NA	NA	0.798	0.547
	Temkin	NA	NA	NA	NA	0.77	1287.54	NA	NA	0.951	0.131
	Dubinin–Raduskevich	NA	4.21	NA	3.21	NA	NA	NA	10.79	0.956	0.117
	Langmuir–Freundlich	0.29	4.16	2.83	NA	NA	NA	NA	NA	0.969	0.084
	Redlich–Peterson	0.58	NA	2.13	NA	NA	NA	0.003	NA	0.851	0.403
Pb(II)	Langmuir	1.37	12.24	NA	NA	NA	NA	NA	NA	0.989	0.056
	Freundlich	7.29	NA	1.59	NA	NA	NA	NA	NA	0.957	0.224
	Temkin	NA	NA	NA	NA	14.93	980.65	NA	NA	0.996	0.020
	Dubinin–Raduskevich	NA	7.82	NA	5.65	NA	NA	NA	2.18	0.996	0.021
	Langmuir–Freundlich	2.42	9.15	1.30	NA	NA	NA	NA	NA	0.995	0.025
	Redlich–Peterson	13.63	NA	1.56	NA	NA	NA	0.96	NA	0.993	0.038

NA: not applicable.

Dubinin–Radushkevich isotherm models as well. The high R^2 values in the Temkin model for the adsorption of Ni(II) and Pb(II) and other parameters of the model such as the equilibrium binding constant (A_T), Temkin isotherm constant (b_T) and the heat of adsorption suggest a physical adsorption process (Table 3).

The Dubinin–Radushkevich isotherm model is used to explain the adsorption mechanism of a heterogeneous surface with a Gaussian energy distribution (E) in terms of physical or chemical adsorption process (Foo and Hameed, 2010; Günay et al., 2007). The mean free energy for Ni(II) and Pb(II) adsorption was 3.21 kJ mol^{-1} and 5.65 kJ mol^{-1}, respectively (Table 3). The mean free energy calculated was less than 8 kJ mol^{-1}, indicating that the adsorption is a physical process (Chathuranga et al., 2014; Huang et al., 2010). The maximum adsorption capacity, q_0, calculated for Pb(II) adsorption varied from the q_0 values calculated from the Langmuir model and Dubinin–Radushkevich model for both Ni(II) and Pb(II) adsorption. Such deviations of q_0 values indicate the unsuitability of two-parameter isotherm model in the biosorption process. Adsorption of Ni(II) and Pb(II) *A. nidus* system cannot be well understood using two-parameter isotherm models.

4.2. Three-parameter isotherm study

Some adsorption systems follow both the Langmuir and the Freundlich isotherms and their adsorption behavior cannot be well explained using these models. To explain such adsorption systems, a combined isotherm model of Langmuir and Freundlich isotherms, which follows the Freundlich isotherm at low adsorbate concentration and the Langmuir isotherm at high adsorbate concentrations is used (Foo and Hameed, 2010; Jeppu and Clement, 2012).

The Redlich–Peterson isotherm is another hybrid model of Langmuir and Freundlich models. It predicts the behavior of the adsorption system with a linear dependence and an exponential dependence on the concentration (Krishna Prasad and Srivastava, 2009; Ng et al., 2002). This model can therefore be used to cover a wide range of concentrations. It was observed that the Langmuir–Freundlich models have high R^2 values (>0.995) for Ni(II) and Pb(II) adsorption. The heterogeneity index calculated from this model for both Ni(II) (2.83) and Pb(II) (1.30) adsorption varied widely (Table 3). Adsorption capacity for Pb(II) is close to the q_0 values predicted by other models (Table 3). However, the q_0 value predicted for Ni(II) adsorption was in agreement with q_0 value predicted by the Dubinin–Radushkevich model but not with the Langmuir model (Table 3). Though the variations were observed in predicted q_0 values in different models high R^2 and low χ^2 suggests that the adsorption system follows the Langmuir–Freundlich isotherm.

The Redlich–Peterson isotherm also predicts the heterogeneity index of the adsorbent surface (Table 3). The predicted value for Ni(II) adsorption was higher than for Pb(II) adsorption. The predicted heterogeneity index for Pb(II) adsorption was closer to the predicted values from the Langmuir–Freundlich model; however, it was closer to the predicted value of the Freundlich model. The difference in heterogeneity of the same biosorbent for two different metal ions can be explained by the hydrated ionic radius of the metal ions. Since the hydrated radius of the Ni(II) ion is larger than that of Pb(II), it covers a comparatively larger area of the biosorbent surface than the Pb(II) ions.

5. Conclusion

Non-living biomass of *A. nidus* leaves adsorb Pb(II) and Ni(II) from aqueous environment. Ni(II) adsorption is enhanced by protonating the biosorbent surface. The maximum adsorption occurs at pH 4–6 and the speed of shaking did not affect adsorption. The kinetics of adsorption follow the pseudo second order kinetic model and the Intraparticle diffusion model suggests that intraparticle diffusion is not the only rate defining step for both Ni(II) and Pb(II) adsorption. Equilibrium data for Pb(II) and Ni(II) follow the combined Langmuir–Freundlich isotherm model. FTIR spectroscopy shows that the hydroxyl, alcohol and amine groups are involved in the adsorption process.

Acknowledgements

The authors express their gratitude to the National Research Council Sri Lanka for their financial support under grant no. NRC 13-087.

References

Akar, T., Celik, S., Gorgulu Ari, A., Tunali Akar, S., 2013. Nickel removal characteristics of an immobilized macro fungus: equilibrium, kinetic and mechanism analysis of the biosorption. J. Chem. Technol. Biotechnol. 88, 680–689.
Amarasinghe, B.M.W.P.K., Williams, R.A., 2007. Tea waste as a low cost adsorbent for the removal of Cu and Pb from wastewater. Chem. Eng. J. 132, 299–309.
Bai, R.S., Abraham, T.E., 2003. Studies on chromium(VI) adsorption–desorption using immobilized fungal biomass. Bioresour. Technol. 87, 17–26.
Chathuranga, P.K.D., Priyantha, N., Iqbal, S.S., Mohomed Iqbal, M.C., 2013. Biosorption of Cr(III) and Cr(VI) species from aqueous solution by *Cabomba caroliniana*: kinetic and equilibrium study. Environ. Earth Sci. 70, 661–671.
Chathuranga, P.K.D., Dissanayake, D.M.R.E.A., Priyantha, N., Iqbal, S.S., Mohamed Iqbal, M.C., 2014. Biosorption and desorption of lead(II) by *Hydrilla verticillata*. Bioremed. J. 18, 192–203.
Dickenson, E.R., Drewes, J., Sedlak, R.E., Wert, D.L., Snyder, E.C.S.A., 2009. Applying surrogates and indicators to assess removal efficiency of trace organic chemicals during chemical oxidation of wastewaters. Environ. Sci. Technol. 43, 6242–6247.
Foo, K.Y., Hameed, B.H., 2010. Insights into the modeling of adsorption isotherm systems. Chem. Eng. J. 156, 2–10.

Günay, A., Arslankaya, E., Tosun, İ., 2007. Lead removal from aqueous solution by natural and pretreated clinoptilolite: adsorption equilibrium and kinetics. J. Hazard. Mater. 146, 362–371.
Ho, Y.-S., 2005. Effect of pH on lead removal from water using tree fern as the sorbent. Bioresour. Technol. 96, 1292–1296.
Ho, Y., McKay, G., 2002. Application of kinetic models to the sorption of copper (II) on to peat. Adsorpt. Sci. Technol. 20, 797–815.
Ho, Y.-S., Wang, C.-C., 2008. Sorption equilibrium of mercury onto ground-up tree fern. J. Hazard. Mater. 156, 398–404.
Huang, L., Zeng, G., Huang, D., Li, L., Huang, P., Xia, C., 2009. Adsorption of lead(II) from aqueous solution onto *Hydrilla verticillata*. Biodegradation 20, 651–660.
Huang, L.-z., Zeng, G.-m., Huang, D.-l., Li, L.-f., Du, C.-y., Zhang, L., 2010. Biosorption of cadmium(II) from aqueous solution onto *Hydrilla verticillata*. Environ. Earth Sci. 60, 1683–1691.
Inglezakis, V.J., Loizidou, M.D., 2007. Ion exchange of some heavy metal ions from polar organic solvents into zeolite. Desalination 211, 238–248.
Inglezakis, V.J., Loizidou, M.D., Grigoropoulou, H.P., 2002. Equilibrium and kinetic ion exchange studies of Pb^{2+}, Cr^{3+}, Fe^{3+} and Cu^{2+} on natural clinoptilolite. Water Res. 36, 2784–2792.
Jacques, R.A., Lima, E.C., Dias, S.L.P., Mazzocato, A.C., Pavan, F.A., 2007. Yellow passion-fruit shell as biosorbent to remove Cr(III) and Pb(II) from aqueous solution. Sep. Purif. Technol. 57, 193–198.
Jeppu, G.P., Clement, T.P., 2012. A modified Langmuir–Freundlich isotherm model for simulating pH-dependent adsorption effects. J. Contam. Hydrol. 129, 46–53.
Krishna Prasad, R., Srivastava, S., 2009. Sorption of distillery spent wash onto fly ash: kinetics and mass transfer studies. Chem. Eng. J. 146, 90–97.
Malkoc, E., Nuhoglu, Y., 2006. Removal of Ni(II) ions from aqueous solutions using waste of tea factory: adsorption on a fixed-bed column. J. Hazard. Mater. 135, 328–336.
Mitra, P., Sarkar, D., Chakrabarti, S., Dutta, B.K., 2011. Reduction of hexa-valent chromium with zero-valent iron: batch kinetic studies and rate model. Chem. Eng. J. 171, 54–60.
Molinari, R., Argurio, P., Poerio, T., 2004. Comparison of polyethylenimine, polyacrylic acid and poly(dimethylamine-co-epichlorohydrin-co-ethylenediamine) in Cu^{2+} removal from wastewaters by polymer-assisted ultrafiltration. Desalination 162, 217–228.
Mondal, M.K., 2009. Removal of Pb(II) ions from aqueous solution using activated tea waste: adsorption on a fixed-bed column. J. Environ. Manag. 90, 3266–3271.
Ng, J., Cheung, W., McKay, G., 2002. Equilibrium studies of the sorption of Cu(II) ions onto chitosan. J. Colloid Interface Sci. 255, 64–74.
Rana, P., Mohan, N., Rajagopal, C., 2004. Electrochemical removal of chromium from wastewater by using carbon aerogel electrodes. Water Res. 38, 2811–2820.
Shroff, K.A., Vaidya, V.K., 2011. Kinetics and equilibrium studies on biosorption of nickel from aqueous solution by dead fungal biomass of *Mucor hiemalis*. Chem. Eng. J. 171, 1234–1245.
Taty-Costodes, V.C., Fauduet, H., Porte, C., Ho, Y.S., 2005. Removal of lead (II) ions from synthetic and real effluents using immobilized *Pinus sylvestris* sawdust: adsorption on a fixed-bed column. J. Hazard. Mater. 123, 135–144.
Volesky, B., 2003. Sorption and Biosorption. BV Sorbex Inc., Montreal.
Volesky, B., Weber, J., Park, J.M., 2003. Continuous-flow metal biosorption in a regenerable *Sargassum* column. Water Res. 37, 297–306.